Progress In Electromagnetics Research M, Vol. 77, 177–186, 2019

Precise Analysis on Paraxial Magnetic Field of Solenoid with Relaxation Polarization Medium

Zhiyong Yang*, Wei Cai, Zhili Zhang, and Youan Xu

Abstract—This paper studies distribution characteristics of paraxial magnetic field of solenoid with inner relaxation polarization medium and driven by ac signal. Firstly, the paraxial electromagnetic field model of hollow solenoid was constructed by Maxwell equations, and the influence of the driving signal frequency was analyzed. Then, based on the established paraxial electromagnetic field model of hollow solenoid, the magnetic field model of solenoid with inner relaxation polarization medium was established by ampere loop law. Finally, the effects of relaxation polarization medium and driving signal frequency on magnetic field amplitude and phase shift were analyzed in detail. The conclusions were drawn as follows: driving signal frequency affects magnetic field amplitude; the relaxation polarization medium will cause the phase shift of magnetic field; and the phase shift will increase as the driving signal frequency increases.

1. INTRODUCTION

Magneto-optical modulation technology has been widely used in fields like laser gyros and high-precision measurement [1, 2], among which the precise analysis on paraxial magnetic field of solenoid driven by ac signal is critically important because it is directly related to the accuracy of magneto-optical modulation.

Most of the current studies on magnetic field of solenoid focus on the following two points: (a) Analysis on the distribution characteristics of magnetic field of solenoid with different methods, such as the calculation of magnetic field of the central solenoid model coil for China Fusion Engineering Experimental Reactor, analysis on the magneto hydrodynamic heat shield system for hypersonic vehicles, magnetic field analysis of solenoid driven by square wave signal, and so on [3–10]. (b) System optimal design based on the analysis of magnetic field of solenoid, such as design and analysis on magnetic field configuration of electromagnetic coil launcher, analysis and optimization of magnetic field of solenoid in magnetic lifting device prototype, analysis and optimization design of coil magnetic field in linear inductance micrometer, etc. [11–15]. It can be seen that there are a few researches on paraxial magnetic field of solenoid driven by ac signal. Only [16] presents a brief analysis on the whole magnetic field of solenoid driven by ac signal, without an accurate elaboration of paraxial magnetic field.

In this paper, the paraxial electromagnetic field model of hollow solenoid driven by ac signal was established by Maxwell equation, and the influence of driving signal frequency on magnetic field was analyzed. Based on the established electromagnetic field model, the magnetic field model of the solenoid with inner relaxation polarization medium was established. Finally, the effects of relaxation polarization medium and driving signal frequency on magnetic field amplitude and phase shift were analyzed in detail.

Received 16 October 2018, Accepted 3 January 2019, Scheduled 11 January 2019
* Corresponding author: Zhiyong Yang (yangzhiyong121@126.com).
The authors are with the Xi'an Research Institute of High-tech, China.

2. PARAXIAL ELECTROMAGNETIC FIELD MODEL OF HOLLOW SOLENOID

2.1. Basic Model

Figure 1 shows the established cylindrical coordinate system of solenoid. The center of the solenoid is the origin. The central axis is Z axis. The positive direction of Z axis and the direction of driving current meet the right-hand helix relationship, and the current is equivalent to surface current.

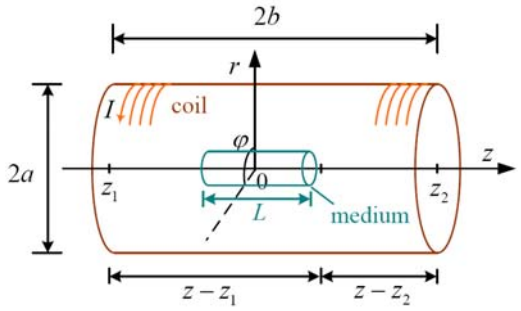

Figure 1. The established cylindrical coordinate system of solenoid, where the radius is a, length is $2b$, turns is N, driving current is I, and the coil density is $n = N/2b$.

The driving current is $I_s = I_m e^{-i\omega t}$, a sine wave signal with magnitude I_m and frequency ω. Solenoid is axisymmetric, so there is no circumferential magnetic field B_φ, axial electric field E_z or radial electric field E_r. Then the electromagnetic field of solenoid is as follows

$$\begin{aligned} \mathbf{B}(r,z,t) &= B_r(r,z,t)\ \mathbf{r} + B_z(r,z,t)\ \mathbf{z} \\ \mathbf{E}(r,z,t) &= E_\varphi(r,z,t)\ \varphi \end{aligned} \tag{1}$$

where $\mathbf{B}$ and $\mathbf{E}$ represent the magnetic field and electric field; B_r and B_z refer to the radial and axial components of the magnetic field; E_φ is the circumferential component of the electric field; r represents the distance from radial direction to central axis; and t is the time.

The space time-varying electromagnetic field based on Maxwell equation is as follows

$$\begin{aligned} \nabla \times \mathbf{E} &= -\frac{\partial \mathbf{B}}{\partial t} \\ \nabla \times \mathrm{H} &= \mathbf{J} + \frac{\partial \mathbf{D}}{\partial t} \\ \nabla \cdot \mathbf{D} &= \rho \\ \nabla \cdot \mathbf{B} &= 0 \end{aligned} \tag{2}$$

where $\mathbf{J}$ is the current density, ρ is the charge density, $\mathbf{D} = \varepsilon_0 \mathbf{E}$ the electric displacement vector, ε_0 the vacuum dielectric constant, $\mathbf{B} = \mu_0 \mathbf{H}$, and μ_0 the vacuum permeability.

Inside the solenoid, $\mathbf{J} = 0$ and $\rho = 0$, we put Eq. (1) into Eq. (2) and obtain the expressions of magnetic field and electric field

$$\frac{\partial E_\varphi}{\partial z} = -\mathrm{i}\omega B_r \tag{3}$$

$$\frac{1}{r}\frac{\partial (rE_\varphi)}{\partial r} = -\mathrm{i}\omega B_z \tag{4}$$

$$\frac{\partial B_r}{\partial z} - \frac{\partial B_z}{\partial r} = -\mathrm{i}\omega\mu_0\varepsilon_0 E_\varphi \tag{5}$$

The magneto-optical material is placed in the central axis attachment of solenoid, and more attention should be paid to the paraxial magnetic field (If there is no special explanation, all the following discussions refer the magnetic field distribution in the magneto-optical material region inside the solenoid as the paraxial magnetic field.). Because magneto-optical material is small and is placed

on the axis of solenoid, and the solenoid is axisymmetric, the radial magnetic field B_r can be neglected when analyzing the paraxial magnetic field, then we acquire the electromagnetic field model as follows

$$r^2\frac{\partial^2 B_z}{\partial r^2}+r\frac{\partial B_z}{\partial r}+k_0^2r^2B_z=0 \tag{6}$$

$$r^2\frac{\partial^2 E_\varphi}{\partial r^2}+r\frac{\partial E_\varphi}{\partial r}+\left(k_0^2r^2-1\right)E_\varphi=0 \tag{7}$$

where the wave vector in vacuum is $k_0=\omega\sqrt{\mu_0\varepsilon_0}=\omega/c$, and c is the speed of light.

2.2. Construction of Paraxial Electromagnetic Field Model of Hollow Solenoid

According to Eq. (6), we acquire the axial magnetic field B_z inside the solenoid as follows

$$B_z(r)=AJ_0(k_0r)+CN_0(k_0r) \tag{8}$$

where A and C are the integral constants; $J_0(k_0r)$ is the first kind of zero-order Bessel function; and $N_0(k_0r)$ is the second kind of zero-order Bessel function.

Because $B_z(\omega\to 0)=AJ_0(k_0r\to 0)+CN_0(k_0r\to 0)=B_0$, $J_0(k_0r\to 0)=1$, and $N_0(k_0r\to 0)=-\infty$, $A=B_0$ and $C=0$, then the axial magnetic field is as follows

$$B_z(r,t)=B_0J_0(k_0r)\cdot e^{-\mathrm{i}\omega t} \tag{9}$$

where B_0 is the magnetic field of solenoid driven by dc signal.

With the method mentioned above, circumferential electric field inside the solenoid is obtained as follows

$$E_\varphi(r)=A'J_1(k_0r)+C'N_1(k_0r) \tag{10}$$

where A' and C' are integral constants; $J_1(k_0r)$ is the first kind of first-order Bessel function; and $N_1(k_0r)$ is the second kind of first-order Bessel function. $C'=0$, when $\omega\to 0$, $J_1(k_0r\to 0)=0$, and $N_1(k_0r\to 0)=-\infty$. The value of A' is determined by the following formula

$$\mathbf{E}=\frac{\mathrm{i}}{\omega\mu\varepsilon}\nabla\times\mathbf{B}=-\frac{\mathrm{i}}{\omega\mu\varepsilon}\frac{\mathrm{d}B}{\mathrm{d}r}e_\varphi \tag{11}$$

According to Eqs. (9), (10) and (11), we acquire $A'=\mathrm{i}cA$ and obtain the expression for the circumferential electric field inside the solenoid as follows

$$E_\varphi(r,t)=\mathrm{i}cB_0J_1(k_0r)\cdot e^{-\mathrm{i}\omega t} \tag{12}$$

According to the magnetic field model in Eq. (9) and the electric field model in Eq. (12), it can be seen that the paraxial electromagnetic field is closely related to the frequency of driving signal and test point position. Fig. 2(a) shows the relationship between magnetic field amplitude and driving signal frequency, and Fig. 2(b) shows the relationship between electric field amplitude and driving signal frequency. The two curves in the same figure show two test points $r=1\,\mathrm{cm}$ and $r=2\,\mathrm{cm}$.

The amplitude of magnetic field in Fig. 2(a) hardly changes, because the driving signal frequency is less than 100 MHz, and the additional magnetic field excited by low frequency alternating electric field is weak. When the driving signal frequency is high, the amplitude of magnetic field attenuates obviously, which is caused by the magnetic field excited by high frequency alternating electric field. According to the comparison of two curves in the same figure, it can be seen that the magnetic field amplitude attenuates with the increase of driving signal frequency, but the magnetic field attenuates faster at a farther test point ($r=2\,\mathrm{cm}$), which means that the magnetic field near the central axis is insensitive to the driving signal frequency.

Both curves in Fig. 2(b) show an increasing trend from zero, signifying that there is electric field excited by alternating magnetic field, and the amplitude of electric field increases with the increase of driving signal frequency. The electric field far from the axis changes faster, indicating the closer to the axis of solenoid, the better the stability of electromagnetic field.

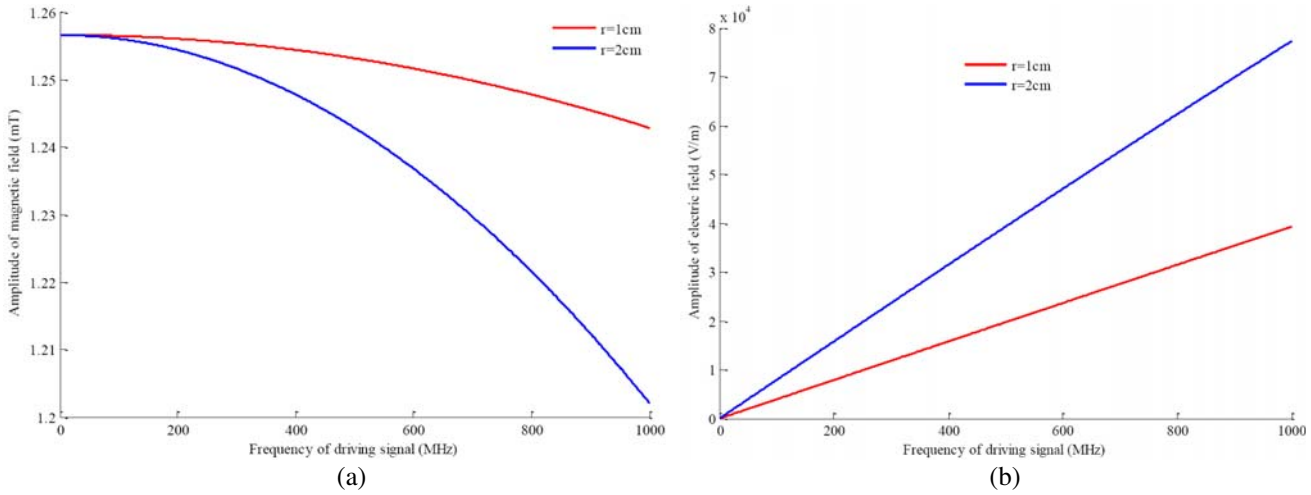

Figure 2. Relationship between electromagnetic field amplitude and driving signal frequency. (a) Magnetic field with driving signal frequency, (b) electric magnetic field with driving signal frequency.

3. PARAXIAL MAGNETIC FIELD OF SOLENOID WITH INNER RELAXATION POLARIZATION MEDIUM

When there is relaxation polarization medium inside the solenoid, the relationship between the electric field frequency and the relaxation time should be taken into account. When the electric field frequency is low, its variation period is longer than relaxation time, and there is no relaxation polarization phenomenon. With the increase of driving signal frequency, the period of electric field becomes shorter. When the electric field period is equal to or shorter than the relaxation time, the relaxation polarization progress will lag behind the variation of electric field, which will result in phase shift. Hence the influence of the phase shift should be taken into consideration when there is relaxation polarization medium inside the solenoid.

Figure 3 shows the magnetic field of solenoid. Its field region is divided into three domains with the boundary of medium and coil. Domain I ($r < R$) presents the magnetic field B_{zr}^{in}, electric field $E_{\varphi r}^{in}$ and phase shift ϕ_i of inner medium. Domain II ($R < r < a$) presents the magnetic field B_{zo}^{in}, electric field $E_{\varphi o}^{in}$ and phase shift ϕ of inner solenoid and outside medium. Domain III ($r > a$) presents the magnetic field B_{zo}^{out}, electric field $E_{\varphi o}^{out}$ and phase shift ϕ_o outside of solenoid.

The progress of establishing electromagnetic field model is the same as the above method, but due to the relaxation polarization medium, the phase shift parameter is added here. Hence the magnetic

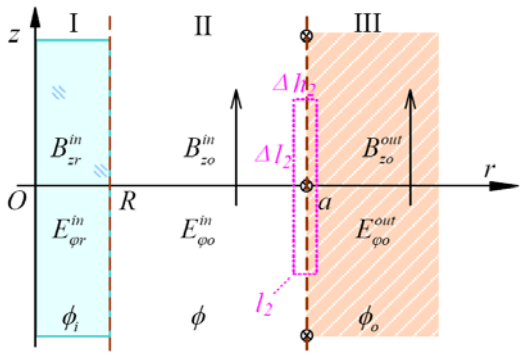

Figure 3. Division of solenoid electromagnetic field.

field expression is acquired as follows

$$\begin{aligned} B_{zr}^{in}(r,t) &= B_0 J_0(kr)\, e^{-\mathrm{i}(\omega t+\phi_i)} \quad (r<R) \\ B_{zo}^{in}(r,t) &= A J_0(k_0 r)\, e^{-\mathrm{i}(\omega t+\phi)} \quad (R<r<a) \\ B_{zo}^{out}(r,t) &= C \mathrm{H}_0^1(k_0 r)\, e^{-\mathrm{i}(\omega t+\phi_o)} \quad (r>a) \end{aligned} \tag{13}$$

According to the electromagnetic relation presented in expression (11), the electric field expression is obtained by applying a similar method.

$$\begin{aligned} E_{\varphi r}^{in}(r,t) &= (\mathrm{i}\omega B_0/k)\, J_1(kr)\, e^{-\mathrm{i}(\omega t+\phi_i)} \quad (r<R) \\ E_{\varphi o}^{in}(r,t) &= (\mathrm{i}\omega A/k_0)\, J_1(k_0 r)\, e^{-\mathrm{i}(\omega t+\phi)} \quad (R<r<a) \\ E_{\varphi o}^{out}(r,t) &= (\mathrm{i}\omega C/k_0)\, \mathrm{H}_1^1(k_0 r)\, e^{-\mathrm{i}(\omega t+\phi_o)} \quad (r>a) \end{aligned} \tag{14}$$

where A and C are the integral constants; $\mathrm{H}_0^1(k_0 r)$ is the first kind of zero-order Hankel function; $\mathrm{H}_1^1(k_0 r)$ is the first kind of first-order Hankel function, satisfying $\mathrm{H}_v^1(x) = J_v(x) + \mathrm{i}N_v(x)$, in which $J_v(x)$ is the first kind of v-order Bessel function; $N_v(x)$ is the second kind of v-order Bessel function; k and k_0 are the wave vectors in medium and air, respectively.

3.1. Magnetic Field Parameter Solution

At the solenoid coil boundary ($r = a$), a narrow rectangular box is taken as the closed integration path l_2, as shown in the dotted frame of Fig. 3. There is current in the area contained by the integral path l_2, and we obtain the expression according to the Ampere loop law

$$\oint_{l_2} B \cdot \mathrm{d}l = \Delta l_2 \left[B_{zo}^{in}(k_0 a) - B_{zo}^{out}(k_0 a) \right] = \mu_0 n I \cdot \Delta l_2 \tag{15}$$

$$B_{zo}^{in}(k_0 a) - B_{zo}^{out}(k_0 a) = \mu_0 n I = B_\infty \tag{16}$$

where n is the coil density.

At the boundary of the medium ($r = R$), there is $B_{zr}(R) - B_{zo}(R) = 0$, then the magnetic field boundary condition can be written as

$$\begin{aligned} B_{zr}^{in}(kR) - B_{zo}^{in}(k_0 a) &= 0 \\ B_{zo}^{in}(k_0 a) - B_{zo}^{out}(k_0 a) &= B_\infty \end{aligned} \tag{17}$$

3.2. Electric Field Parameter Solution

The electromagnetic induction law is introduced here.

$$\oint_l E \cdot \mathrm{d}l = -\int_S \frac{\partial B}{\partial t} \cdot \mathrm{d}S \tag{18}$$

where l and S represent the integral path and the area surrounded by the path, respectively. A very narrow ring frame ($\Delta h' \to 0$) is selected along the coil boundary as integration path l' as shown in Fig. 4.

Electromagnetic induction law is applied to the integration path

$$\oint_l E \cdot \mathrm{d}l = \left[E_{\varphi o}^{in}(k_0 a) - E_{\varphi o}^{out}(k_0 a) \right] \Delta l' = -\frac{\partial B}{\partial t} \cdot \Delta l' \cdot \Delta h' \tag{19}$$

Because $\partial B/\partial t$ is finite, and Eq. (19) goes to zero, $E_{\varphi o}^{in}(k_0 a) - E_{\varphi o}^{out}(k_0 a)$.

The similar conclusion can be drawn by applying electromagnetic induction law at the boundary of medium ($r = R$). Therefore, the electric field boundary conditions can be expressed as

$$\begin{aligned} E_{\varphi r}^{in}(kR) &= E_{\varphi o}^{in}(k_0 R) \\ E_{\varphi o}^{in}(k_0 a) &= E_{\varphi o}^{out}(k_0 a) \end{aligned} \tag{20}$$

According to Eqs. (17) and (20), it can be seen that the circumferential electric field is continuous in the whole space of solenoid, while the axial magnetic field will jump at the coil boundary but is continuous in other spaces.

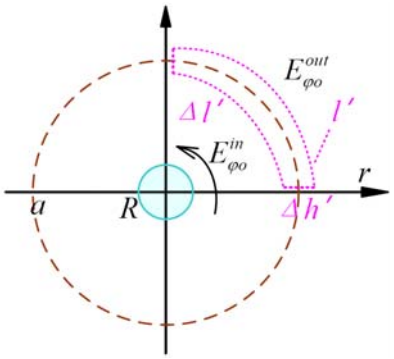

Figure 4. Cross section of solenoid.

3.3. Electromagnetic Field Parameter Solution

According to magnetic field expression (13), magnetic field boundary condition (17), electric field expression (14) and electric field boundary condition (20), we obtain the equation

$$\begin{aligned} &B_0 J_0(kR)\cdot e^{-\mathrm{i}\phi_i} - AJ_0(k_0R)\cdot e^{-\mathrm{i}\phi} = 0 \\ &AJ_0(k_0a)\cdot e^{-\mathrm{i}\phi} - C\mathrm{H}_0^1(k_0a)\cdot e^{-\mathrm{i}\phi_o} = B_\infty \\ &k_0 B_0 J_1(kR)\cdot e^{-\mathrm{i}\phi_i} = kAJ_1(k_0R)\cdot e^{-\mathrm{i}\phi} \\ &AJ_1(k_0a)\cdot e^{-\mathrm{i}\phi} = C\mathrm{H}_1^1(k_0a)\cdot e^{-\mathrm{i}\phi_o} \end{aligned} \tag{21}$$

Equation (21) is solved, and the following parameters are obtained

$$\begin{aligned} \phi_o &= \arctan\left[\frac{QN_0(k_0a) - PN_1(k_0a)}{QJ_0(k_0a) - PJ_1(k_0a)}\right] \\ \delta &= \arctan\left[\frac{N_1(k_0a)}{J_1(k_0a)}\right] \\ \phi_i &= \phi_o - \delta \\ \phi &= \arctan\left[\frac{k_0}{k}\frac{J_0(k_0R)J_1(kR)}{J_0(kR)J_1(k_0R)}\tan\phi_i\right] \\ A &= B_0\frac{J_0(kR)}{J_0(k_0R)}\frac{\cos\phi_i}{\cos\phi} \\ C &= \frac{J_0(k_0a)}{J_0(k_0R)}\frac{\mu_0 nI\cdot\sin\phi_i}{J_0(k_0R)\sin\delta - N_0(k_0R)\cos\delta} \end{aligned} \tag{22}$$

Here $P = \frac{J_0(kR)}{J_0(k_0R)}J_0(k_0a)$, $Q = \frac{k_0}{k}\frac{J_1(kR)}{J_1(k_0R)}J_1(k_0a)$. J_0 and J_1 are the first kind of zero-order and the first-order Bessel function, respectively. N_0 and N_1 are the second kind of zero-order and the first-order Bessel function, respectively.

4. CHARACTERISTICS ANALYSIS ON MAGNETIC FIELD

4.1. Frequency Characteristics of Magnetic Field Amplitude

Simulation parameters are as follows: $I_m = 1\,\mathrm{A}$, $n = 1000$, $a = 3.5\,\mathrm{cm}$, $b = 5.5\,\mathrm{cm}$, $L = 3\,\mathrm{cm}$, $R = 1\,\mathrm{cm}$, $\varepsilon_r = 4.1$, $\mu_r = 1$, test points are $r = 0.5R$ and $r = 2R$. Fig. 5 shows the effect of driving signal frequency on magnetic field amplitude at different test points.

The solid line in Fig. 5 represents the magnetic field of solenoid with relaxation polarization medium, in which the dotted line is the magnetic field without relaxation polarization medium; the red curve

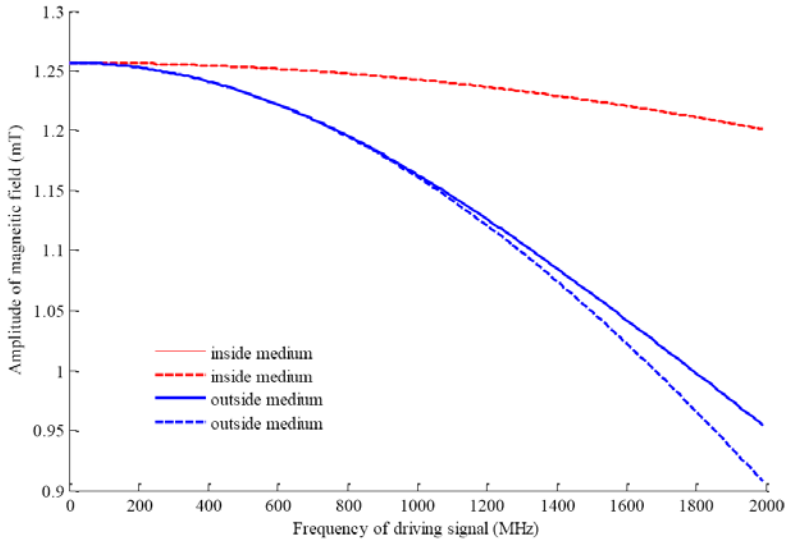

Figure 5. Magnetic field frequency characteristics of solenoid with relaxation polarization medium.

indicates the magnetic field at the test point $r = 0.5R$; the blue curve indicates the magnetic field at the test point $r = 2.0R$. The solid and dotted lines of red curves in Fig. 5 almost coincide, which means that the relaxation polarization medium does not affect the magnetic field amplitude of inner medium. The blue curves indicate that with the frequency increase of driving signal, the solid line and dotted line gradually separate, and the higher the frequency is, the greater the difference between the two curves will be. Therefore, the relaxation polarization medium affects the magnetic field outside the medium and slows down the attenuation of the magnetic field.

4.2. Magnetic Field Distribution Characteristics

The simulation parameters remain unchanged. The two specific frequencies of driving signal are 100 MHz and 500 MHz, respectively. The distribution of magnetic field in radial direction is shown in Fig. 6.

The solid line in Fig. 6 shows the distribution of the magnetic field of solenoid with relaxation

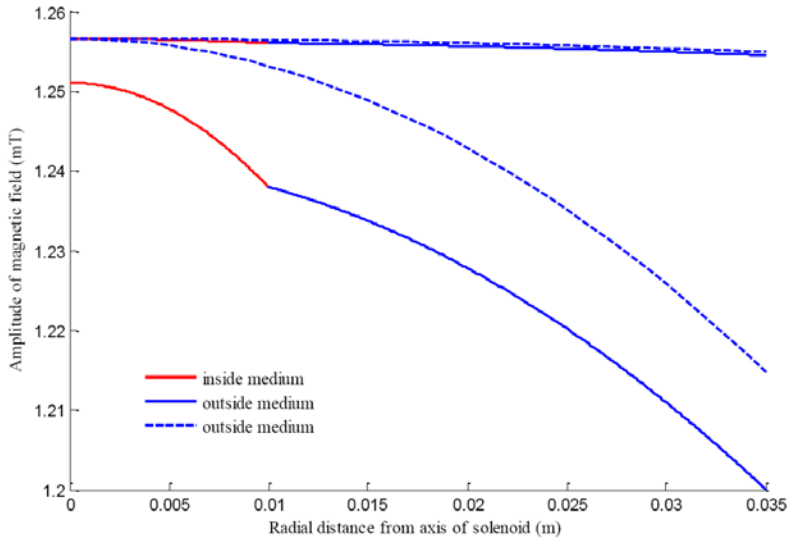

Figure 6. Distribution of magnetic field in solenoid with or without relaxation medium.

polarization medium. The dotted line represents the distribution of the magnetic field without relaxation polarization medium. The red part of solid line refers to the magnetic field inside the medium, and the blue curve is the magnetic field outside the medium. From Fig. 6 we observe that when there is relaxation polarization medium in the solenoid, and the driving signal frequency is high, there is a downward displacement about the magnetic field, which is the effect of the phase shift caused by relaxation polarization medium.

4.3. Analysis on Magnetic Field Phase Shift

The phase shift is introduced in the polarization process, which causes a series of changes. The high frequency electric field related with driving signal leads to the phase shift, and the electric field is from driving signal, so the phase shift is closely related to the frequency of driving signal. Fig. 7 describes the variation of magnetic field phase shift with the change of driving signal frequency. With the increase of driving signal frequency, the phase shift is going to be negative gradually, and the variation rate becomes larger and larger.

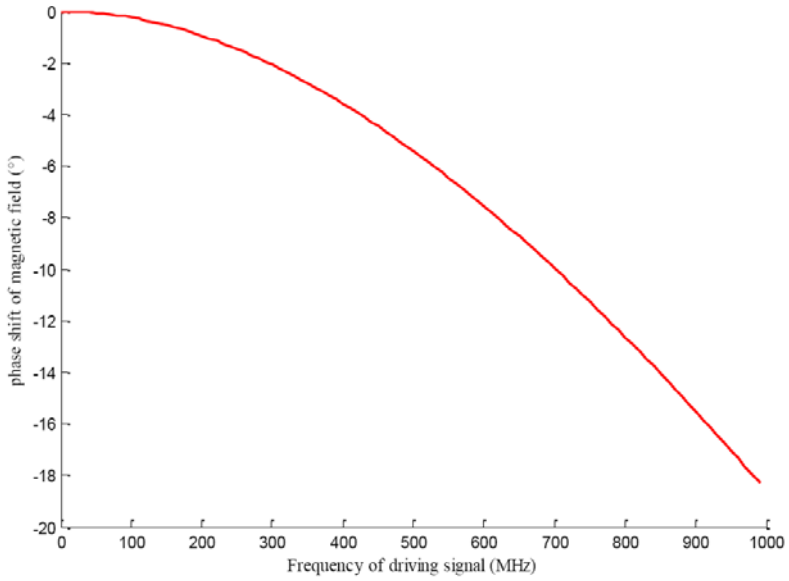

Figure 7. Phase shift of magnetic field in solenoid with driving signal frequency.

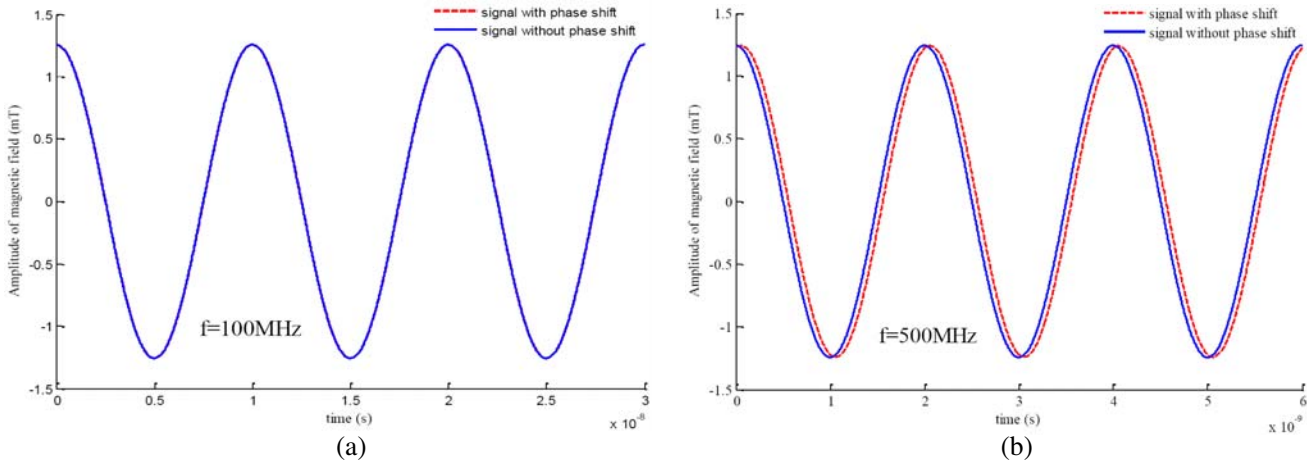

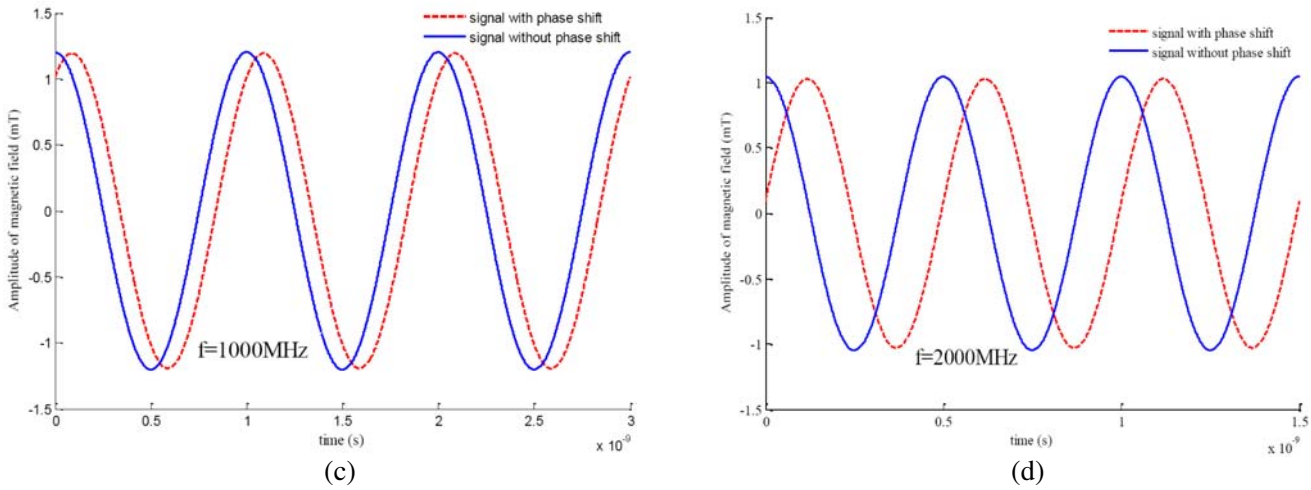

Figure 8. Effect of driving signal frequency on magnetic field in solenoid.

4.4. Analysis on the Influence of Driving Signal Frequency

The simulation parameters remain unchanged, and the test point is $r = 2$ cm. Fig. 8 shows the effect of driving signal frequency on magnetic field, and the frequencies of driving signal in Figs. 8(a), (b), (c), and (d) are 100 MHz, 500 MHz, 1000 MHz, and 2000 MHz, respectively. The red curve represents the magnetic field of solenoid with relaxation polarization medium, and the blue curve represents the magnetic field of hollow solenoid.

It can be found from Fig. 8(a) that the two curves coincide when the frequency of driving signal is low, which proves that there is no change of magnetic field or phase shift. From the comparison with Figs. 8(b), (c) and (d), it can be seen that with the increase of driving signal frequency, the magnetic field amplitude decreases, and the phase shift increases, indicating that high frequency driving signal causes the change of magnetic field. The higher the frequency is, the more significant the change will be.

5. CONCLUSION

In this research, the magnetic field characteristics of solenoid with relaxation polarization medium and driven by sine wave signal was studied based on Maxwell equation and Ampere loop theorem. The magnetic field models of hollow solenoid and solenoid with relaxation polarization medium were established respectively, and the effects of relaxation polarization medium and driving signal frequency on magnetic field and phase shift were analyzed. The conclusions are obtained as follows:

a) The frequency of driving signal affects the amplitude of magnetic field. The higher the signal frequency is, the more obvious the attenuation of magnetic field amplitude will be.

b) The medium in solenoid will affect the distribution of magnetic field, and the relaxation polarization medium will delay the attenuation of magnetic field outside the medium.

c) Relaxation polarization medium causes phase shift of magnetic field, and the phase shift increases with the increase of driving signal frequency.

ACKNOWLEDGMENT

This study was supported by the National Natural Sciences Foundation of China (grant No. 61505254).

REFERENCES

1. Wang, Z. G., X. W. Long, and F. Wang, "Zero drift sensitivity in four-frequency differential laser gyros," *Infrared and Laser Engineering*, Vol. 40, 1758–1762, Sep. 2011.
2. Shang, H. N., W. Quan, Y. Chen, Y. Li, and H. Li, "The measuring method of atomic polarization of alkali metal vapor based on optical rotation and the analysis of the influence factors," *Spectroscopy and Spectral Analysis*, Vol. 36, 305–309, Feb. 2016.
3. Peng, L., Z. H. Yang, Q. Hu, T. Huang, and B. Li, "Finite element computation of 2-D magnetic field of solenoid with current," *High Power Laser and Particle Beams*, Vol. 23, 2151–2156, Aug. 2011.
4. Cai, W., F. C. Wu, Z. Y. Yang, Y. G. Hou, and J. H. Xing, "Analysis of solenoid magnetic field based on Maxwell equation," *High Power Laser and Particle Beams*, Vol. 27, 123201, Dec. 2015.
5. Cai, W., F. C. Wu, and Z. Y. Yang, "Magnetic field of long solenoid driven by square wave," *Laser & Optoelectronics Progress*, Vol. 52, 092601, Sep. 2015.
6. Liang, M. L. and K. Xue, "Calculation of the magnetic field of the finite solenoid with a rectangular cross section," *Physics and Engineering*, Vol. 28, 57–61, Jan. 2018.
7. Liao, B., C. F. Deng, X. Y. Wu, X. Zhang, A. D. Liu, and H. Liang, "Inner magnetic field distribution of solenoid studied by matlab," *Journal of Beijing Normal University (Natural Science)*, Vol. 46, 688–690, Jun. 2010.
8. Fang, Y. Z., Q. M. Xu, J. J. Zheng, B. H. Lv, R. M. Pan, H. Q. Ye, et al., "Investigation on the relation between tne length of magnetic core and the giant magnetoimpedance effect of solenoid with FeCo-based magnetic core," *Acta Phys. Sin.*, Vol. 60, 127501, Dec. 2011.
9. Li, K. and W. Q. Liu, "Analysis of the magnetohydrodynamic heat shield system for hypersonic vehicles," *Acta Phys. Sin.*, Vol. 65, 064701, Jun. 2016.
10. Ji, F., S. J. Du, X. G. Liu, and Z. L. Wang, "Magnetic field and electromagnetic load calculation for CFETR central solenoid model coil," *Journal of Hefei University of Technology*, Vol. 38, 788–792, Jun. 2015.
11. Lü, L., "Improvement of precision for linear inductance micrometer," *Optics and Precision Engineering*, Vol. 23, 191–196, Jan. 2015.
12. Zhu, Y. W., H. T. Li, Z. M. Yan, L. Fu, and Y. Wang, "Design and analysis for magnetic field configuration of electromagnetic coil launcher," *Acta Armamentarii*, Vol. 32, 464–468, Apr. 2011.
13. Zhao, L. X., M. B. Lü, X. Zhang, H. Y. Yu, Q. G. Yao, G. Q. Liu, et al., "Numerical analysis and experimental study of the magnetic lifting device prototype," *High Power Laser and Particle Beams*, Vol. 27, 076003, Jul. 2015.
14. Wu, W., Z. J. Wang, B. M. Wu, S. F. Han, D. S. Ni, E. M. Mei, et al., "Development of a surperconducting solenoid for CADS," *Chinese Physics C*, Vol. 38, 017003, Jan. 2014.
15. Li, P., Y. Z. Liu, and J. L. Wang, "Port magnetic flux leakage suppression technology for static magnetic system of nuclear magnetic resonance gyroscope," *Journal of Chinese Inertial Technology*, Vol. 26, 56–62, Jan. 2018.
16. Gerald, S. H., "The high-frequency electric and magnetic fields of a solenoid," *Journal of Applied Physics*, Vol. 69, 7400–7405, Nov. 1991.